

The black hole mass – stellar velocity dispersion correlation: bulges versus pseudobulges

Jian Hu

Max-Planck-Institut für Astrophysik, Karl-Schwarzschild-Straße 1, D-85741 Garching bei München, Germany
Email: jhu@mpa-garching.mpg.de

Accepted ... Received ...; in original form ...

ABSTRACT

We have investigated the correlation between the supermassive black holes (SMBHs) mass (M_{bh}) and the stellar velocity dispersion (σ_*) in two types of host galaxies: the classical bulges (or elliptical galaxies), and pseudobulges. In the form $\log(M_{\text{bh}}/M_{\odot}) = \alpha + \beta \log(\sigma_*/200 \text{ km s}^{-1})$, the best-fit results for the 41 classical bulges/elliptical galaxies are the slope $\beta = 4.10 \pm 0.25$ and the normalization $\alpha = 8.29 \pm 0.04$; the best-fit results for the 12 pseudobulges are $\beta = 4.17 \pm 0.73$, $\alpha = 7.49 \pm 0.13$. Both relations have intrinsic scatter in $\log M_{\text{bh}}$ of $\lesssim 0.25$ dex. The $M_{\text{bh}}\text{-}\sigma_*$ relation for pseudobulges is different from the relation in the classical bulges over the 3σ significance level. The contrasting relations indicate the formation and growth histories of SMBHs depend on their host type, the pseudobulges is relatively low efficient to fuel the central SMBHs. The discrepancy between the slope of the $M_{\text{bh}}\text{-}\sigma_*$ relations using different definition of velocity dispersion vanishes in our sample, a uniform slope will constrain the coevolution theories of the SMBHs and their host galaxies more effectively. We also find the slope for the 13 “core” elliptical galaxies at the high mass range of the relation appears slightly steeper, which may be the imprint of their origin of dissipationless mergers.

Key words: black hole physics – galaxies: bulges – galaxies: formation – galaxies: fundamental parameters – galaxies: nuclei.

1 INTRODUCTION

Supermassive black holes (SMBHs) are ubiquitous in the center of elliptical galaxies and bulges of disk galaxies. The masses (M_{bh}) of the nearby mostly quiescent SMBHs are found to be correlated with the physical properties of their host bulges, such as the luminosity L (Kormendy & Richstone 1995; Marconi & Hunt 2003), the mass M_{b} (Magorrian et al. 1998; Marconi & Hunt 2003; Häring & Rix 2004), the stellar velocity dispersion σ_* (Ferrarese & Merritt 2000; Gebhardt et al. 2000a; Tremaine et al. 2002; Ferrarese & Ford 2005), the galaxy light concentration C_{Re} (Graham et al. 2001), the Sérsic index n of surface brightness profile (Graham & Driver 2007), and the inner core radius r_{γ} (Lauer et al. 2007a). Among these, the $M_{\text{bh}}\text{-}\sigma_*$ relation of the form

$$\log(M_{\text{bh}}/M_{\odot}) = \alpha + \beta \log(\sigma/200 \text{ km s}^{-1}) \quad (1)$$

is one of the most tight with a intrinsic scatter of $\lesssim 0.3$ dex (Novak et al. 2006). The validity of this relation have been explored for intermediate mass black holes (IMBHs) in dwarf galaxies (Barth et al. 2005), the local active galaxies (McLure & Dunlop 2002; Green & Ho 2006), and Seyfert galaxies at $z = 0.36$ (Woo et al. 2006; Treu et al. 2007). As a crucial test of theoretical models of formation and coevolution of the SMBHs and their host galaxies, many efforts have been made to reproduce the slope of the relation (e.g.

Silk & Rees 1998; King 2003). The normalization, intrinsic scatter, and redshift-dependent evolution of the relation are important for study of SMBHs demography (e.g. Yu & Tremaine 2002; Shankar et al. 2004).

The early published estimation of the slope β are diverse from the highest value 4.8 ± 0.5 (Ferrarese & Merritt 2000, hereafter FM00) to the lowest value 3.75 ± 0.3 (Gebhardt et al. 2000a, hereafter the Nukers). Tremaine et al. (2002, hereafter T02) explored the reasons for the discrepancy between the results of the two groups, and show the systematic differences in the velocity dispersion measurements contribute the main diversity in the slope. The Nukers define “effective stellar velocity dispersion” σ_e as the luminosity-weighted rms dispersion within a slit aperture of length $2R_e$, while FM00 use “central stellar velocity dispersion” σ_c normalized to a aperture of radius $R_e/8$, where R_e is the effective radius of the galaxy bulges. T02 presented a best-fit result of the $M_{\text{bh}}\text{-}\sigma_e$ relation with $\alpha = 8.13 \pm 0.06$ and $\beta = 4.02 \pm 0.32$, which is extensively used in the subsequent studies. The most current version of the $M_{\text{bh}}\text{-}\sigma_c$ relation are $\alpha = 8.22 \pm 0.06$ and $\beta = 4.86 \pm 0.43$ (Ferrarese & Ford 2005, hereafter FF05). Although both of the relations are tight, their slopes still differ by 1.6 standard deviations.

Besides the uncertainty in slope and normalization, the de-

pendence of the $M_{\text{bh}}-\sigma_*$ relation on the type of SMBHs host is also worth consideration. A variety of observational and theoretical results show that there are two kinds of central component in disk galaxies (cf. review, e.g. Kormendy & Kennicutt 2004). The classical bulges dwelling in the center of (mostly) early-type disk galaxies are like little elliptical galaxies, which are thought to be the products of violent relaxation during major mergers. On the other hand, pseudobulges in (mostly) late-type disk galaxies are physically unrelated to ellipticals, their structure and kinematics resemble that of disks. They are believed to have formed via distinct scenario than that of classical bulges. There is no guarantee that SMBHs in pseudobulges should follow the same $M_{\text{bh}}-\sigma_*$ relation in ellipticals. In contrast, several evidences suggest they probably obey a different relation. (i) The rotationally flattened pseudobulges have smaller velocity dispersion than predicted by the Faber-Jackson σ_*-L correlation. If the pseudobulge follow the same $M_{\text{bh}}-L$ relation, they will naturally deviate from the same $M_{\text{bh}}-\sigma_*$ relation. (ii) The pseudobulges are dominantly shaped by the secular evolution, and probably never undergo a major merger, which is postulated as the key mechanism to explain the $M_{\text{bh}}-\sigma_*$ relation in the ellipticals. The gas inflow fueling SMBHs induced by the secular evolution is not as effective as that in major merger events. (iii) The slope of the $M_{\text{bh}}-\sigma_*$ relation in the local active galactic nuclei (AGNs) flattens somewhat at the low mass end (Greene & Ho 2006). Because most of the local low mass AGNs have late-type hosts (Kauffmann et al. 2003), we speculate some (or even most) of these low mass SMBHs may live in the pseudobulges, and disagree with the relation for high mass AGNs with (mostly) early-type hosts.

Kormendy & Gebhardt (2001) have checked five pseudobulges, and found no obvious inconsistency with the relation for the ellipticals. However, one of these galaxies, NGC 4258, was in fact a classical bulge, incorrectly identified as a pseudobulge (J. Kormendy, private communication), and is consistent with the $M_{\text{bh}}-\sigma_*$ relation for the elliptical galaxies, while the M_{bh} of the other four pseudobulges appears smaller than the prediction by the relation (cf. Fig. 5 of Kormendy & Gebhardt 2001). As pointed out by the authors, it is important to check their result with a larger sample. Therefore, in this paper, we investigate the $M_{\text{bh}}-\sigma_*$ relation with the up-to-date sample of classical bulges¹ and pseudobulges.

The paper is organized as follows. In section 2, we describe the sample used for analysis. In section 3, we determine and compare the $M_{\text{bh}}-\sigma_*$ relation in classical bulges and pseudobulges. In section 4, we summarize and discuss our results. Throughout this paper, we use the base 10 logarithms, and cosmological constants $\Omega_M = 0.3$, $\Omega_\Lambda = 0.7$, $h = 0.7$.

2 THE SAMPLE

We select the sample with spatially well-resolved M_{bh} measurement from literature, and classify them as classical bulges or pseudobulges. The selection criteria is $2r_{\text{bh}}/r_{\text{res}} > 1$, where $r_{\text{bh}} = GM_{\text{bh}}/\sigma_*^2$ is the radius of the SMBHs influence sphere, r_{res} is the instrumental spatial resolution (e.g. for *HST*, $r_{\text{res}} \approx 0''.07$). In order to improve the statistics of the poor sampled pseudobulges, we add three SMBHs with mass measurement by reverberation mapping (RM). The agreement between the mass measurements by RM

¹ In the following part of this paper, we call classical bulges including the elliptical galaxies.

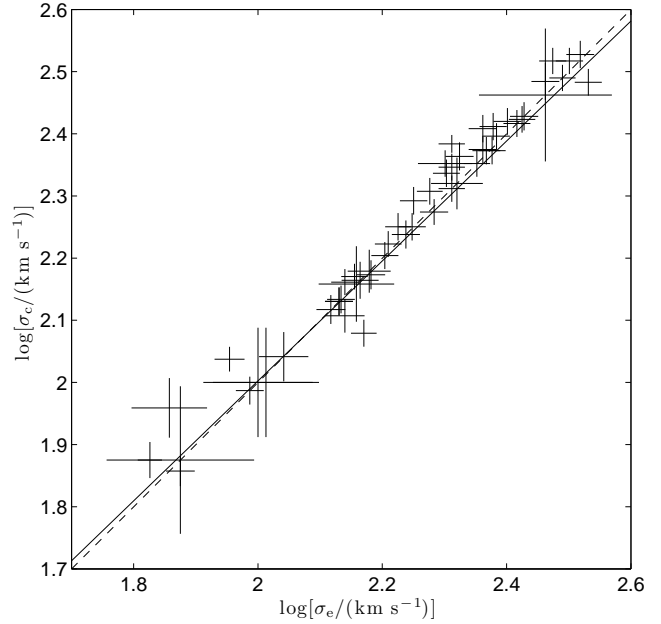


Figure 1. Comparison of the σ_e and σ_c of the sample galaxies. The solid line denotes the model of T02 (eq. [2]). The dashed line denotes $\sigma_e = \sigma_c$.

method and stellar/gas dynamics have been demonstrated in the cases of NGC 3227 and NGC 4151. The M_{bh} estimated by RM method² is accurate within a factor of 3 with no additional systematic errors (e.g. uncertainties in distance, inclination, mass to light ratio, etc.).

The properties of the bulges and SMBHs are listed in Table 1 and Table 2. Our sample (41 classical bulges + 12 pseudobulges) is larger than T02 (31 galaxies) and FF05 (30 galaxies), with updated mass and/or velocity dispersion measurement. Among the 53 objects, 30 are weighted by stellar dynamics, 15 by gas dynamics (3 have both stellar and gas dynamics measurements), 6 by masers, 1 by stellar proper motions, and 3 by RM; 22 are inactive, 16 are LINERs, 6 are Seyfert 1, and 9 are Seyfert 2.

Most distances of galaxies in the sample have been measured with the surface brightness fluctuation (SBF) method (Tonry et al. 2001). The distances to the galaxies in Virgo cluster (NGC 4459, NGC 4473, NGC 4486, NGC 4486A, NGC 4552, NGC 4564, NGC 4649) are based on the new SBF measurement by Mei et al. (2007). For those without an SBF distance we use recession velocities corrected for Virgocentric infall from HyperLeda database, except some individual galaxies explained in section 2.2. The black hole mass is corrected according to the modified distance that is different from the value used in the literature describing the mass measurement.

Most of the velocity dispersions σ_c are calculated using the formula $\sigma_c = \sigma_{c0}(8R_{\text{ap}}/R_e)^{0.04}$ (Jørgensen, Franx, & Kjaergaard 1995), where σ_{c0} are provided by the HyperLeda database, $R_{\text{ap}} =$

² In this paper, we use the scaling factor $f = 3$ instead of 5.5 ± 1.8 determined by Onken et al. (2004). The later value was calibrated using $M_{\text{bh}}-\sigma_*$ relation for the elliptical galaxies, which is not proper for the pseudobulges in their sample. We have re-calibrated the factor f , and found the commonly used value 3 is a better choice for both the classical bulges and pseudobulges (Hu, in preparation). In the subsequent analysis, we use 0.5 dex errors in $\log M_{\text{bh}}$ of the RM objects to account for the possible uncertainty of f .

Table 1. The sample of black holes in classical bulges and elliptical galaxies.

Galaxy	Type	Activity	D (Mpc)	M_{\bullet} ($10^8 M_{\odot}$)	ref	σ_e (km s^{-1})	σ_c (km s^{-1})	ref	n	R_e (kpc)	ref
(1)	(2)	(3)	(4)	(5)	(6)	(7)	(8)	(9)	(10)	(11)	(12)
N221	E2	n	0.81	0.025 ± 0.005	s-48	75 ± 4	72 ± 4^a	46	3.7	0.24	38, 34
N224	Sb	L	0.76	$1.4^{+0.9}_{-0.3}$	s-4	160 ± 8	160 ± 8	46	2.2	1.0	31
N821	E4	n	24.1	0.85 ± 0.35	s-39	189 ± 9	203 ± 10^a	8	4.0	5.23	17
N1399 ^c	E1	n	21.1	12^{+5}_{-6}	s-30	317 ± 16	329 ± 16^a	30	4.9	4.1	40
N2974	E4	Sy2	21.5	1.7 ± 0.3	s-9	233 ± 12	236 ± 12^a	8	4.1	2.5	8
N3031	Sab	L	3.9	$0.8^{+0.2}_{-0.1}$	g-15	173 ± 9^a	173 ± 9^a		2.0	0.21	33
N3115	S0	n	9.7	9.2 ± 3.0	s-16	230 ± 12	256 ± 13^a	46	4.4	4.7	38, 34
N3227	SBa	Sy1	17.5	$0.20^{+0.14}_{-0.13}$	s-12,g-29	136 ± 7	136 ± 7	35	2.2	0.15	33
N3245	S0	L	20.9	2.1 ± 0.5	g-2	205 ± 10	222 ± 11^a	46	4.0	1.08	17
N3377	E5	n	11.2	0.7 ± 0.1	s-11	138 ± 7	145 ± 7^a	8	3.0	2.38	17
N3379 ^c	E1	L	10.6	$2.0^{+2.0}_{-1.5}$	s,g-22	201 ± 10	217 ± 11^a	8	4.3	2.2	24, 8
N3414	S0	n	25.2	2.5 ± 0.4	s-9	205 ± 10	242 ± 12^a	8	3.8	4.0	38, 8
N3608 ^c	E2	L	22.9	$1.9^{+1.0}_{-0.6}$	s-23	178 ± 9	196 ± 10^a	8	4.9	4.6	38, 8
N3998	S0	L	18.3	$2.9^{+2.6}_{-2.2}$	s-13	268 ± 14	268 ± 14	49	4.1	0.70	13
N4151	Sa	Sy1	13.9	$0.3^{+0.1}_{-0.2}$	s-31,g-29	97 ± 5	97 ± 5	35	3.0	0.32	21
N4258	Sb	L	7.2	0.39 ± 0.01	m-28	148 ± 7	120 ± 6	3	3.0	3.1	42
N4261 ^c	E2	L	31.6	$5.2^{+1.0}_{-1.1}$	g-19	309 ± 15^a	309 ± 15^a		3.8	6.5	38, 34
N4291 ^c	E2	n	26.2	$3.1^{+0.8}_{-2.3}$	s-23	242 ± 12	249 ± 12^a	23	4.6	2.04	17
N4459	S0	L	16.1	0.70 ± 0.13	g-41	168 ± 8	178 ± 9^a	8	3.5	3.0	38, 8
N4473 ^c	E5	n	15.3	$1.1^{+0.4}_{-0.8}$	s-23	192 ± 10	188 ± 9^a	8	2.7	2.1	24, 8
N4486 ^c	E0	L	17.2	30 ± 10	g-25	298 ± 15	329 ± 16^a	8	6.9	8.8	24, 8
N4486A	E2	n	18.3	0.14 ± 0.09	s-36	110 ± 10^b	110 ± 10^b		2.2	0.54	36, 18
N4552 ^c	E	L	15.9	5.0 ± 0.8	s-9	252 ± 13	263 ± 13^a	8	4.8	2.4	38, 8
N4564	S0	n	15.9	$0.59^{+0.03}_{-0.08}$	s-23	162 ± 8	167 ± 8^a	43	3.2	1.54	24, 23
N4596	SB0	n	16.7	$0.78^{+0.42}_{-0.33}$	g-41	152 ± 8	149 ± 8^a	41	1.4	0.23	33
N4621	E5	n	18.3	4.0 ± 0.6	s-9	211 ± 11	231 ± 12^a	8	5.2	4.1	38, 8
N4649 ^c	E1	n	17.3	20^{+4}_{-6}	s-23	330 ± 17^b	337 ± 17^a		6.0	6.13	24, 23
N4697	E4	n	11.7	$1.7^{+0.2}_{-0.3}$	s-23	177 ± 9	178 ± 9^a	23	4.0	4.25	24, 23
N4742	S0	n	15.5	$0.14^{+0.04}_{-0.05}$	s-46	90 ± 5	109 ± 5^a	46	5.9	0.60	38
N5077 ^c	E3	L	40.2	$7.2^{+4.5}_{-3.0}$	g-14	261 ± 13^a	261 ± 13^a		4.7	3.8	14
N5128	S0	Sy2	3.5	$0.45^{+0.17}_{-0.10}$	g-27	138 ± 10	128 ± 8^a	43	4.0	1.4	43
N5252	S0	Sy2	96.8	10^{+15}_{-5}	g-5	209 ± 20	209 ± 20	10	6.0	9.7	6, 34
N5813 ^c	E1	L	32.2	7.0 ± 1.1	s-9	230 ± 12	237 ± 12^a	8	4.9	8.1	38, 8
N5845	E3	n	25.9	$2.4^{+0.4}_{-1.4}$	s-23	239 ± 12	258 ± 13^a	8	3.2	0.58	24, 8
N5846	E0	n	24.9	11 ± 2	s-9	238 ± 12	236 ± 12^a	8	3.9	9.8	35, 8
N6251	E2	Sy2	107	$6.1^{+2.0}_{-2.1}$	g-20	290 ± 15	305 ± 21^a	46	4.0	11	34
N7052 ^c	E4	L	71.4	$4.0^{+2.8}_{-1.6}$	g-47	266 ± 13	265 ± 13^a	47	4.6	12	24, 34
N7332	SB0	n	23.0	$0.13^{+0.06}_{-0.05}$	s-26	135 ± 7	135 ± 7	32	3.9	1.2	38, 32
N7457	S0	n	13.2	$0.035^{+0.011}_{-0.014}$	s-23	67 ± 3	75 ± 5^a	23	2.0	0.22	1
Cyg A	E	Sy1	240	25 ± 7	g-44	290 ± 70^a	290 ± 70^a	45	...	31	34
IC 1459 ^c	E3	L	29.2	25^{+5}_{-4}	s-7	340 ± 17	304 ± 15^a	7	4.9	8.2	34

Notes: Column (1), name of the galaxy. Column (2), Hubble type of the galaxy. Column (3), the activity of the galactic nuclei (n = inactive; Sy1 = Seyfert 1; Sy2 = Seyfert 2; L = LINER). Column (4), distance to the galaxy. Column (5), mass of the central black hole. Column (6), method (s = stellar dynamics; g = gas dynamics; m = H₂O masers; p = stellar proper motions) and reference for the black hole mass measurement. Column (7-9), effective and central stellar velocity dispersion of the bulge, and their references. Column (10-12), Sérsic index and effective radius of the bulge surface brightness profile, and their references.

^a The value is taken from HyperLeda database, corrected with the aperture of R_e (if available), the relative error is taken as 5%.

^b The value is estimated by the author, see details in section 2.2.

^c The “core” elliptical galaxies (Lauer et al. 2007a).

References: (1) Balcells, Graham & Peletier 2007; (2) Barth et al. 2001; (3) Batcheldor et al. 2005; (4) Bender et al. 2005; (5) Capetti et al. 2005; (6) Capetti & Balmaverde 2007; (7) Cappellari et al. 2002; (8) Cappellari et al. 2006; (9) Cappellari et al. 2007b; (10) Cid Fernandes et al. 2004; (11) Copin et al. 2004; (12) Davies et al. 2006 (13) De Francesco et al. 2006; (14) De Francesco et al. 2008; (15) Devereux et al. 2003; (16) Emsellem et al. 1999; (17) Erwin et al. 2002; (18) Faber et al. 1989; (19) Ferrarese et al. 1996; (20) Ferrarese & Ford 1999; (21) Gadotti 2007; (22) Gebhardt et al. 2000b; Shapiro et al. 2006; (23) Gebhardt et al. 2003; (24) Graham & Driver 2007; (25) Harms et al. 1994; Macchetto et al. 1997; (26) Häring & Rix 2004; (27) Häring-Neumayer et al. 2006; Neumayer et al. 2007; (28) Herrnstein et al. 1999; (29) Hicks & Malkan 2008; (30) Houghton et al. 2006; Gebhardt et al. 2007; (31) Kormendy & Bender 1999; (32) Kuntschner et al. 2006; (33) Laurikainen et al. 2004; Laurikainen et al. 2005; (34) Marconi & Hunt 2003; (35) Nelson et al. 2004; (36) Nowak et al. 2007; (37) Onken et al. 2007; (38) Prugniel & Héraudeau 1998; (39) Richstone et al. 2004; (40) Saglia et al. 2000; (41) Sarzi et al. 2001; (42) Scarlata et al. 2004; (43) Silge et al. 2005; (44) Tadhunter et al. 2003; (45) Thornton et al. 1999; (46) Tremaine et al. 2002; (47) van den Bosch & van der Marel 1995; (48) Verolme et al. 2002; (49) Wegner et al. 2003.

Table 2. The sample of black holes in pseudobulges.

Galaxy	Type	Activity	D (Mpc)	M_{\bullet} ($10^8 M_{\odot}$)	ref	σ_e (km s^{-1})	σ_c (km s^{-1})	ref	n	R_e (kpc)	ref
(1)	(2)	(3)	(4)	(5)	(6)	(7)	(8)	(9)	(10)	(11)	(12)
N1023	SB0	n	11.4	0.44 ± 0.05	s-3	205 ± 10	205 ± 10^a	3	2.01	1.2	12, 18
N1068	Sb	Sy2	15.0	0.083 ± 0.003	m-17	151 ± 12	151 ± 12	19	1.69	3.1	6, 18
N2787	SB0	L	7.5	$0.41^{+0.04}_{-0.05}$	g-22	200 ± 20^b	225 ± 11^a		1.0	0.32	7
N3079	SBcd	Sy2	19.1	0.025 ± 0.005	m-24	146 ± 10^a	146 ± 10^a		
N3384	SB0	n	11.6	$0.16^{+0.01}_{-0.02}$	s-10	143 ± 7	148 ± 7^a	23	1.0	1.2	7
N4945	SBcd	Sy2	3.8	0.014 ± 0.003^c	m-13	100 ± 20^b	100 ± 20^b		
Circinus	Sb	Sy2	2.8	0.011 ± 0.002	m-14	75 ± 20	75 ± 20	2	
IC 2560	SBb	Sy2	39.3	0.042 ± 0.008^c	m-16	144 ± 20	144 ± 20	4	...	0.34	8
MW	SBbc	n	0.008	0.037 ± 0.002	p-11	103 ± 20	100 ± 20	23	1.32	0.7	12, 23
N4051	SBbc	Sy1	22.4	0.010 ± 0.004	r-21	72 ± 10	91 ± 10	1	2.0	0.34	6
N4593	SBb	Sy1	35.3	0.053 ± 0.011	r-5	135 ± 7	135 ± 7	20	0.9	1.1	9
N7469	SBa	Sy1	70.8	0.066 ± 0.008	r-21	131 ± 7	131 ± 7	20	...	1.8	20

Notes: Similar as Table 1. Three SMBHs with mass measurement by reverberation mapping (RM) are denoted by ‘r’ in column (6), their mass uncertainties listed in the table are only due to the RM measurements.

^a The value is taken from HyperLeda database, corrected with the aperture of R_e (if available), the relative error is taken as 5%.

^b The value is estimated by the author, see details in section 2.2.

^c The mass uncertainty is absent in the literature, we take the relative value of 20% as a rough estimation.

References: (1) Batcheldor et al. 2005; (2) Bian & Gu 2007; (3) Bower et al. 2001; (4) Cid Fernandes et al. 2004; (5) Denney et al. 2006; (6) Drory & Fisher 2007; (7) Erwin et al. 2002; (8) Fathi & Peletier 2003; (9) Gadotti 2007; (10) Gebhardt et al. 2003; (11) Ghez et al. 2005; (12) Graham & Driver 2007; (13) Greenhill et al. 1997; (14) Greenhill et al. 2003; (15) Hicks & Malkan 2007; (16) Ishihara et al. 2001; (17) Lodato & Bertin 2003; Greenhill & Gwinn 1997; (18) Marconi & Hunt; (19) Nelson & Whittle 1995; (20) Nelson et al. 2004; (21) Peterson et al. 2004; (22) Sarzi et al. 2001; (23) Tremaine et al. 2002; (24) Yamauchi et al. 2004; Kondratko, Greenhill, & Moran 2005.

0.85 kpc, R_e is the effective radius of bulges surface brightness profile, listed in the column (11) of Table 1 and 2. Follow T02, we adopt relative errors in σ_e and σ_c of 5%, except for some individual galaxies explained in section 2.2. For those without σ_e in literature, we take the value of σ_e , since they are very close on average. T02 have modeled the σ_e - σ_c relation for 39 early-type galaxies, and found (cf. eq. [16] in T02):

$$\log(\sigma_c/\sigma_e) = (-0.008 \pm 0.004) - (0.035 \pm 0.017) \log(\sigma_c/200 \text{ km s}^{-1}). \quad (2)$$

Comparison of the σ_e and σ_c of our sample galaxies is shown in Figure 1. Obviously, the difference between the σ_e and σ_c are much smaller than their measurement errors.

2.1 Identification of pseudobulges

A comprehensive review on the pseudobulge properties and methods to recognize pseudobulges are tabulated in Kormendy & Kennicutt (2004). Sérsic index $n < 2$ is a simple but not safe criteria for pseudobulges (Fisher 2006), which is consistent with the observations of our sample. Morphology and kinetic property are more reliable indicators than Sérsic index. In general, if the “bulge” contains a nuclear bar, nuclear spiral, and/or nuclear ring, the bulge is identified as a pseudobulge. In $(V_{\text{max}}/\sigma_b)$ - ϵ diagram, pseudobulges locate above the oblate rotator line (Binney 1978; 2005), where V_{max} is the maximum line-of-sight rotational velocity of the bulge, σ_b is the stellar velocity dispersion of the bulge just outside the nucleus, and ϵ is the characteristic ellipticity in the region interior to the radius of V_{max} .

NGC 1023 is a galaxy with two nested bars, and the nuclear bar identifies the bulge as pseudo-type (J. Kormendy, private communication). The complex kinematics of the HI in the galaxy suggests that significant accretion of gas has occurred recently (Oosterloo et al. 2007).

NGC 1068 and NGC 4051 have been morphologically identified as pseudobulges using *HST* optical images by Drory & Fisher (2007).

NGC 2787 has a spectacular tilted nuclear dust ring of radius $\sim 1.''5$ - $10''$ (Sarzi et al. 2001; Erwin et al. 2003). NGC 3384 has a bulge with disk-like kinetic property, $(V_{\text{max}}/\sigma_b)=0.77$, $\epsilon=0.29$ (de Zeeuw et al. 2002). NGC 2787 and NGC 3384 are examples of the galaxies contain composite structures consisting of both pseudobulges and small inner classical bulges (Erwin 2007).

NGC 3079 has a peanut-shaped bulge (Lütticke, Dettmar, & Pohlen 2000), which shows the cylindrical rotation (Shaw, Wilkinson & Carter 1993), a character of disklike pseudobulge.

NGC 4945 has a box-shape bulge (Lütticke, Dettmar, & Pohlen 2000). The CO studies present a nuclear gas ring (Ott et al. 2001).

The inner region of Circinus galaxy is bluer than typical bulge, that indicate young stellar populations (Wilson et al. 2000). The existence of a nuclear ring in CO emission (Curran et al. 1998) and near-UV light (Muñoz Marín et al. 2007) identify the pseudobulge.

IC 2560 has a box-shape bulge (Lütticke, Dettmar, & Pohlen 2000). The red-shifted features in the H_2O maser emission are slightly stronger than the blue-shifted, which is a typical characteristic seen in most megamasers and may be explained by a spiral structure of the maser-emitting nuclear disk (Ishihara et al. 2001).

The classification of the bulge of our Galaxy is ambiguous. The observation that it is box shaped strongly favors a pseudobulge, but the stellar population age and α -element overabundance are most easily understood if the bulge is classical (Kormendy & Kennicutt 2004). The Sérsic index $n = 1.32$ is disklike. In this paper, we tentatively take the Milky way as a pseudobulge.

NGC 4593 contains a nuclear ring of dust, has been identified as a pseudobulge by Kormendy et al. (2006).

NGC 7469 has strong, ring like nuclear emission from star

formation region (Knapen et al. 2006; Muñoz Marín et al. 2007), which marks the pseudobulge.

Most of the pseudobulges in our sample dwell in the barred galaxies (10/12), and most of our sample galaxies contain classical bulge are unbarred (14/17). In the end, we caution that the identification of pseudobulges is still somewhat uncertain, some galaxies need further discrimination.

2.2 Comments on individual objects

Classical bulges:

NGC 221 (M32).—It is a small, low-luminosity elliptical, has a main body of Sérsic profile with index $n < 4$ and extra light near the center above the inward extrapolation of the outer Sérsic function (Kormendy 1999).

NGC 3227.—The mass $2.0^{+1.4}_{-1.3} \times 10^7 M_\odot$ is a mean value of the measurement using stellar dynamics ($[0.7-2.0] \times 10^7 M_\odot$, Davies et al. 2006) and gas dynamics ($2.3^{+1.1}_{-0.5} \times 10^7 M_\odot$ [corrected for distance], Hicks & Malkan 2008), which is consistent with the RM measurement ($[2.3 \pm 1.2] \times 10^7 M_\odot$, Peterson et al. 2004).

NGC 4151.—The mass $3^{+1}_{-2} \times 10^7 M_\odot$ is a mean value of the measurement using stellar dynamics ($\sim 4 \times 10^7 M_\odot$, Onken et al. 2007) and gas dynamics ($3.2^{+0.8}_{-2.3} \times 10^7 M_\odot$ [corrected for distance], Hicks & Malkan 2008), which is consistent with the RM measurement ($2.49^{+0.31}_{-0.26} \times 10^7 M_\odot$, Bentz et al. 2006).

NGC 4486A.—We estimate the velocity dispersion according to the Figure 4 in Nowak et al. (2007).

NGC 4596.—The Sérsic index $n = 1.4$ of the bulge is disk-like (Laurikainen et al. 2005), but the kinetic property ($V_{\text{max}}/\sigma_b = 0.3$, $\epsilon = 0.15$) is elliptical, the stellar population is also old (Peletier et al. 2007).

NGC 4649.—We estimate the σ_e using the stellar velocity dispersion profile measured by Bridges et al. (2006).

NGC 5128.—The distance is taken as average of value derived from different methods (Rejkuba 2004; Karachentsev et al. 2007; Ferrarese et al. 2007).

NGC 7332.—This galaxy has a boxy bulges (Lütticke, Dettmar, & Pohlen 2000; Kormendy & Kennicutt 2004). The kinetic property ($V_{\text{max}}/\sigma_b = 0.32$, $\epsilon = 0.42$) identifies it as a classical bulge (Cappellari et al. 2007a).

NGC 7457.—This galaxy has a young box-shape bulge (Lütticke, Dettmar, & Pohlen 2000; Kormendy & Kennicutt 2004). Kormendy (1993) suggest it as a pseudobulge according to its small σ_* . But the kinetic property ($V_{\text{max}}/\sigma_b = 0.62$, $\epsilon = 0.44$) identifies it as a classical bulge (Cappellari et al. 2007a).

Pseudobulges:

NGC 2787.—T02 gives $\sigma_e = 140 \text{ km s}^{-1}$, while in the literature much higher value are quoted, e.g., 210 km s^{-1} (Dalle Ore et al. 1991), 205 km s^{-1} (Neistein et al. 1999), 202 km s^{-1} (Barth et al. 2002), and 257 km s^{-1} (Erwin et al. 2003). As pointed by Aller et al. (2007), this discrepancy may stem from the central peak in the velocity dispersion profile (cf. e.g., Fig. 1 of Bertola et al. 1995). Follow Aller et al. (2007), we estimate $\sigma_e = 200 \pm 20 \text{ km s}^{-1}$.

NGC 3079.—The accretion disk of the SMBH is probably thick, flared, and clumpy, in contrast to the compact, thin, warped, differentially rotating disk in the archetypal maser galaxy NGC 4258 (Kondratko, Greenhill, & Moran 2005). The mass of SMBH thus may be underestimated.

NGC 4945.—The velocity dispersion is estimate by author from the maximum circular velocity (V_c)-central velocity disper-

sion (σ) relation for the Scd type galaxies (Courteau et al. 2007), where $V_c = 167 \text{ km s}^{-1}$ is taken from the Hyperleda database.

The distances to NGC 4945 and Circinus galaxy are taken from Karachentsev et al. (2007).

We do not include the following galaxies in our sample:

NGC 1300 and NGC 2748.—The masses of SMBHs in NGC 1300 ($6.6^{+6.3}_{-3.2} \times 10^7 M_\odot$) and NGC 2748 ($4.4^{+3.5}_{-3.6} \times 10^7 M_\odot$) are measured with nuclear gas kinetics by Atkinson et al. (2005). They neglected the effect of extinction by dust in the analysis of the gaseous rotation curves. The extinction in the H band which was used to measure the black hole masses yield an underestimation in luminosity of $\sim 20\%$ for NGC 1300 and $\sim 58\%$ for NGC 2748 in their central 50 pc regions. Therefore, the M_{bh} of the two galaxies are probably overestimated. Their results are much higher than the prediction of $M_{\text{bh}}-\sigma_*$ or $M_{\text{bh}}-L$ relations ($7 \times 10^6 M_\odot$ or $2 \times 10^7 M_\odot$ for NGC 1300; $6 \times 10^6 M_\odot$ or $7 \times 10^6 M_\odot$ for NGC 2748). In fact, the *HST* can only barely resolved the sphere of influence of SMBHs with the mass predicted by the $M_{\text{bh}}-\sigma_*$ or $M_{\text{bh}}-L$ relations ($r_{\text{bh}} = 0''.04 \sim 0''.1$ for NGC 1300; $r_{\text{bh}} = 0''.03$ for NGC 2748). NGC 1300 has spiral-like dust lanes down to the center, wrapping around the nucleus (Scarlata et al. 2004), and connecting to the leading edge of a strong kpc-scale bar (Martini et al. 2003), which suggests gas inflow in both large and small scale. The bulge of NGC 1300 is disk-like with Sérsic index $n = 1.3$ (Laurikainen et al. 2004), and identified as a pseudobulge by Kormendy & Fisher (2005). The nuclei of N2748 is not well defined in *HST* observations due to dust lane obscuration (Scarlata et al. 2004). The surface brightness profile in the central region show evidence of nuclear cluster (Hughes et al. 2005), which may also indicates the existence of a pseudobulge.

NGC 2778 and NGC 4303.—*HST* cannot resolve the influence radius of the SMBHs in NGC 2778 ($2r_{\text{bh}}/r_{\text{res}} = 0.8$, Gebhardt et al. 2003) and in NGC 4303 ($2r_{\text{bh}}/r_{\text{res}} = 0.9$, Pastorini et al. 2007). The zero black hole mass model for NGC 2778 is ruled out at only the 95% confidence limit (Gebhardt et al. 2003).

NGC 4342.—The mass of the central SMBH measured by Cretton & van den Bosch (1999) make this object a outlier for the $M_{\text{bh}}-L$ relation (Marconi & Hunt 2003) and the $M_{\text{bh}}-M_b$ relation (Häring & Rix 2004). According to the analysis of Valluri, Merritt & Emsellem (2004), no best-fit value of M_{bh} can be found for this object, the published value $3.0^{+1.7}_{-1.0} \times 10^8 M_\odot$ is probably overestimated.

NGC 4374.—As pointed by T02, the published measurement of M_{bh} in NGC 4374 (M84) is differ from each other beyond the stated errors.

NGC 7582.—The influence radius of the SMBH is not well resolved, $2r_{\text{bh}}/r_{\text{res}} = 0.7$ (Wold et al. 2006).

The more reliable and accurate mass measurement of these SMBHs in the future will contribute to the poorly sampled low-mass end of the $M_{\text{bh}}-\sigma_*$ relation, especially for the pseudobulges.

3 THE ESTIMATION OF $M_{\text{BH}}-\sigma_*$ RELATIONS

3.1 The linear fitting algorithm

Different authors use different algorithms to estimate the log-linear $M_{\text{bh}}-\sigma_*$ relation eq. (1). The Nukers and T02 fit the relation by minimizing “ χ^2 estimator”

$$\chi^2 = \sum_{i=1}^N \frac{(y_i - \alpha - \beta x_i)^2}{\epsilon_{y_i}^2 + \beta^2 \epsilon_{x_i}^2} \quad (3)$$

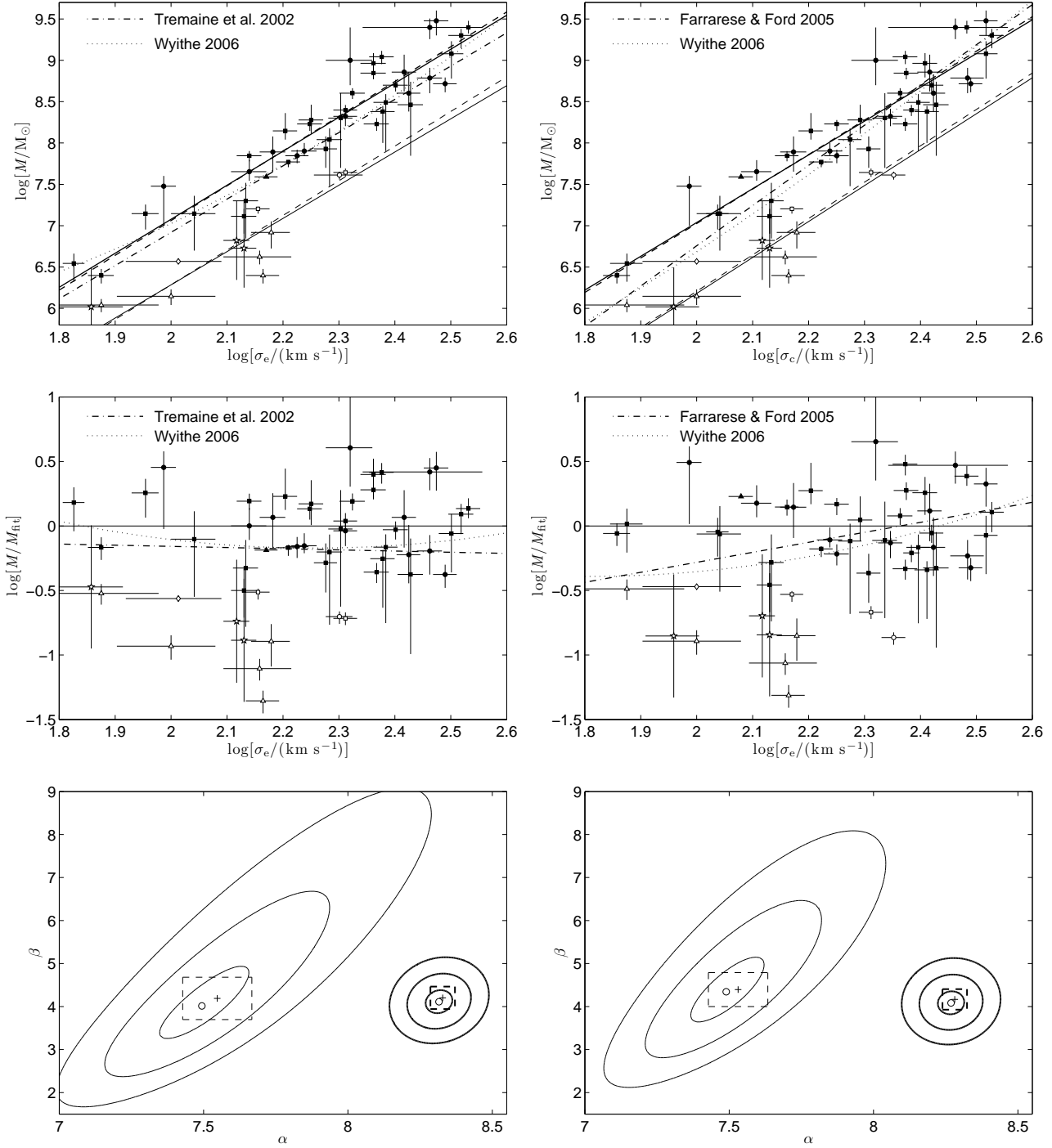


Figure 2. *Left-top:* The $M_{\text{bh}}-\sigma_e$ relations for classical bulges (filled markers, thick lines) and pseudobulges (open markers, thin lines). Mass measurement based on stellar dynamics are denoted by squares, on gas dynamics by circles, on masers by triangles, on stellar proper motions by diamond, and on reverberation mapping by stars. The solid lines are fitting results using χ^2 estimator, dashed lines using AB estimator. The best-fit result of T02 and Wyithe 2006 are plotted for comparison in dash-dotted line and dotted line. *Left-middle:* Residuals between the measured M_{bh} and the prediction by best-fit relation using χ^2 estimator for classical bulges. The markers are the same as the top panel. The differences between the best-fit relation of T02, Wyithe 2006 and our result are plotted in dash-dotted and dotted lines respectively. *Left-bottom:* The contours are 1σ , 2σ and 3σ limits of χ^2 fitting of α and β . The central circles denote best-fit value. The dashed squares and their central cross markers denote the best-fit value and uncertainties using AB estimator. The thick and thin lines are results of classical bulges and pseudobulges respectively. *Right:* Similar as the left panel, but for the $M_{\text{bh}}-\sigma_e$ relations, the best-fit of T02 is substituted by one of FF05.

Table 3. The fitting results of the $M_{\text{bh}}\text{-}\sigma_*$ relation.

Host type	$M_{\text{bh}}\text{-}\sigma_e$					$M_{\text{bh}}\text{-}\sigma_c$				
	α_{χ^2}	β_{χ^2}	ϵ_0	α_{AB}	β_{AB}	α_{χ^2}	β_{χ^2}	ϵ_0	α_{AB}	β_{AB}
classical bulge	8.32 ± 0.04	4.11 ± 0.24	0.25	8.33 ± 0.04	4.20 ± 0.26	8.27 ± 0.04	4.08 ± 0.25	0.25	8.28 ± 0.04	4.17 ± 0.24
pseudobulge	7.49 ± 0.15	4.01 ± 0.78	0.21	7.55 ± 0.12	4.19 ± 0.49	7.49 ± 0.11	4.34 ± 0.68	0.18	7.53 ± 0.10	4.40 ± 0.39
combined	8.19 ± 0.06	4.81 ± 0.32	0.40	8.19 ± 0.05	4.75 ± 0.30	8.14 ± 0.06	4.75 ± 0.32	0.38	8.14 ± 0.05	4.97 ± 0.34
core galaxies	8.29 ± 0.10	4.42 ± 0.76	0.21	8.29 ± 0.08	4.47 ± 0.65	8.18 ± 0.11	4.94 ± 0.78	0.19	8.18 ± 0.07	4.99 ± 0.61
normal ellipticals	8.31 ± 0.06	4.04 ± 0.33	0.27	8.34 ± 0.07	4.22 ± 0.38	8.25 ± 0.06	3.93 ± 0.33	0.27	8.28 ± 0.07	4.09 ± 0.34

(Press et al. 1992), where $x = \log(\sigma/200 \text{ km s}^{-1})$, $y = \log(M_{\text{bh}}/M_{\odot})$, ϵ_{xi} and ϵ_{yi} are errors of x and y measurements. In order to account for the intrinsic scatter in the $M_{\text{bh}}\text{-}\sigma_*$, T02 replace ϵ_{yi} by $(\epsilon_{yi}^2 + \epsilon_0^2)^{1/2}$, where ϵ_0 is a constant denotes the intrinsic scatter of y at a fixed x . The value of ϵ_0 is set so that the best-fit reduced χ^2 is equal to its expectation value of unity, T02 find $\epsilon_0 = 0.27$ for their sample. The 1σ , 2σ , 3σ uncertainties in α and β are given by the upper and lower limits of α and β for which $\chi^2 - \chi_{\text{min}}^2 = 1.01, 6.75, 16.68$.

FF05 use the “AB estimator” described by Akritas & Bershady (1996) to determine the best-fit α , β and their uncertainties. Both χ^2 and AB estimators have the advantages of accounting for measurement uncertainties in both variables and are asymptotically normal and consistent. In our analysis, the AB estimator gives the similar estimate for the slope β (cf. Figure 2, Figure 3, and Table 3). A review of the comparison of the two estimator can be found in T02.

In the subsequent analysis, we use both logarithms to estimate α and β , and denote them as α_{χ^2} , β_{χ^2} and α_{AB} , β_{AB} , respectively.

3.2 The slope and normalization of the relations

The fitting results of the $M_{\text{bh}}\text{-}\sigma_e$ relation and the $M_{\text{bh}}\text{-}\sigma_c$ relation are shown in Figure 2. The best-fit value and uncertainties of α , β and ϵ_0 are summarized in Table 3. We notice the $M_{\text{bh}}\text{-}\sigma_e$ and $M_{\text{bh}}\text{-}\sigma_c$ relations are roughly the same, and the results derived by two fitting algorithms are very close, both within 1σ uncertainty.

The slope β for the classical bulges derived by two fitting algorithms and two dispersion definitions, is in the range of $4.0\sim 4.2$ with uncertainties of ~ 0.25 . It is consistent with but slightly smaller than the result of T02 ($\beta = 4.02 \pm 0.32$). We take the mean fitting results by χ^2 estimator as the “uniform” $M_{\text{bh}}\text{-}\sigma_*$ relation for the classical bulges:

$$\alpha = 8.29 \pm 0.04, \quad \beta = 4.10 \pm 0.25. \quad (4)$$

The case for the pseudobulges are similar, but with the different value. Their best-fit of $M_{\text{bh}}\text{-}\sigma_*$ by χ^2 estimator is

$$\alpha = 7.49 \pm 0.13, \quad \beta = 4.17 \pm 0.73. \quad (5)$$

The intrinsic scatter for the classical bulges and pseudobulges are 0.25 and 0.20 respectively. The M_{bh} measurement and the prediction by the best-fit relation are compared in the middle panels of Figure 2. The best-fits of T02, FF05 and Wyithe 2006 are plotted in the same figures for comparison. Most of the pseudobulges lie below the prediction of relation for the classical bulges and of all the three previous formula.

The discrepancy between the $M_{\text{bh}}\text{-}\sigma_*$ relations for the classical bulges and pseudobulges is explicit in the bottom panels of Figure 2. They are distinct over 3σ significance level. The Kolmogorov-Smirnov test gives a very low probability ($P = 4 \times 10^{-11}$) that the $M_{\text{bh}}\text{-}\sigma_*$ relation for pseudobulge agrees with the relation for the classical bulges.

The relation for the pseudobulges has a similar slope but 0.8 ± 0.1 dex smaller normalization than the relation for the classical bulges. The normalization α derived by T02 are just between our estimates of the classical bulges and pseudobulges, may be a result of fitting for a mixed sample of two kinds of bulges.

We also fit the $M_{\text{bh}}\text{-}\sigma_*$ relation for a combined sample of the total 54 objects, obtain a steeper slope than that of the both samples. It is easy to be understood that, the $M_{\text{bh}}\text{-}\sigma_*$ relation for pseudobulges is roughly parallel but lower than that for classical bulges, the high mass end dominant classical bulges and the low mass end dominant pseudobulges will thus determine a steeper relation for the combined sample. It can partially explain the steep slope derived by FF05 (cf. middle-right panel of Figure 2).

3.3 The $M_{\text{bh}}\text{-}\sigma_*$ relation for the “core” galaxies

Some elliptical galaxies are found to have cores in their central brightness profiles (Lauer et al. 1995). A core is evident as a radius at which the steep envelope of the galaxy breaks and becomes a shallow profile in logarithmic coordinates. The cores are believed formed by binary BHs in the dissipationless (“dry”) mergers. These remnants of dry mergers will preserve the $M_{\text{bh}}\text{-}L$ relation but deviate from the $M_{\text{bh}}\text{-}\sigma_*$ relation, because the Faber-Jackson relationship $L \propto \sigma^7$ for the “core” galaxies are much steeper than the classic $L \propto \sigma^4$ for the “normal” elliptical galaxies (Lauer et al. 2007a). On the other hand, the SMBHs masses M_{bh} predicted by the $M_{\text{bh}}\text{-}\sigma_*$ relation is systematically smaller the masses predicted by the $M_{\text{bh}}\text{-}L$ relation for high-luminosity galaxies, such as brightest cluster galaxies (BCGs). The BCGs have large cores, which are probably formed in the dry mergers. Hence, the $M_{\text{bh}}\text{-}\sigma_*$ relation will break at the high mass range due to the core galaxies made by dry mergers.

Inspired by these arguments, we attempt to compare the $M_{\text{bh}}\text{-}\sigma_*$ relations of 13 core elliptical galaxies in our sample and of the other normal early type galaxies. Figure 3 depict the $M_{\text{bh}}\text{-}\sigma_*$ relations for the core elliptical galaxies and the other normal elliptical galaxies. The best-fit results are presented in Table 3. Two relations are still tight ($\epsilon_0 \lesssim 0.27$), consistent within 1σ uncertainties, but the former is slightly steeper ($\beta \simeq 5.0$) than that later ($\beta \simeq 4.0$). Our result confirms the argument of Lauer et al. (2007a) that the $M_{\text{bh}}\text{-}\sigma_*$ relation derived from all the early type galaxies underestimates the mass of SMBHs in the center of core galaxies statistically. The sub-sample of core galaxies overlap the one of the normal elliptical galaxies in the mass range of $10^8 \sim 10^{10} M_{\odot}$, therefore the intrinsic scatter of the correlation for the combined sample in the high mass range is larger than that in the low mass range.

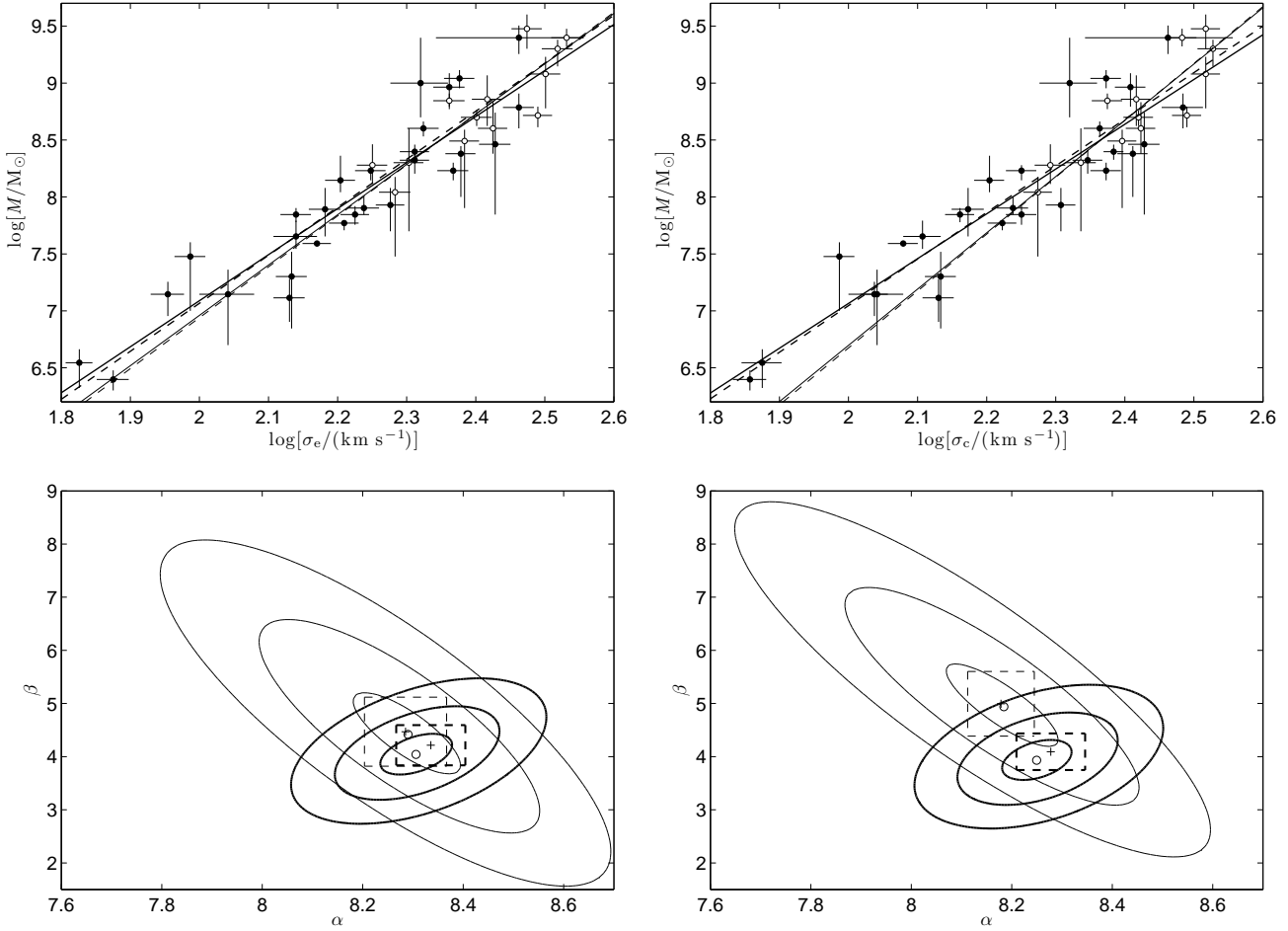


Figure 3. *Left-top:* The best-fit $M_{\text{bh}}-\sigma_e$ relations for “core” galaxies (open circles, thin lines) and the other early-type galaxies (filled circles, thick lines). The solid lines and dashed lines denote fitting results using χ^2 and AB estimator respectively. *Left-bottom:* The contours are 1σ , 2σ and 3σ limits of χ^2 fitting of α and β in eq. (1). The central circles denote best-fit value. The dashed squares and their central cross markers denote the best-fit value and uncertainties using AB estimator. The thin and thick lines are results of “core” galaxies and the normal elliptical galaxies. *Right:* Similar as the left panel, but for the $M_{\text{bh}}-\sigma_c$ relations.

4 CONCLUSIONS AND DISCUSSION

We examine whether classical bulges and pseudobulges obey the same relation between black hole mass and stellar velocity dispersion, using the largest published sample to date. The main conclusions of this paper are as follows:

(1) On the relation for classical bulges, we find a similar slope ($\beta = 4.10 \pm 0.25$) and higher normalization ($\alpha = 8.29 \pm 0.04$) than the previous result of Tremaine et al. (2002). The intrinsic scatter of the relation is $\lesssim 0.25$ dex.

(2) The pseudobulges have their own tight $M_{\text{bh}}-\sigma_*$ relation with $\beta = 4.29 \pm 0.66$, $\alpha = 7.47 \pm 0.11$, which are distinct from the relation for classical bulges over the 3σ significance level.

(3) There is evidence of a steeper slope for the “core” galaxies at high black hole masses end.

The mass density of local SMBHs calculated with the $M_{\text{bh}}-\sigma_*$ relation (e.g. Yu & Tremaine 2002; Wyithe & Loeb 2003; Shankar et al. 2004) is consistent with the cumulative mass density of optical or X-ray selected quasar remnants expected from energy arguments (e.g. Soltan 1982; Fabian & Iwasawa 1999; Yu & Tremaine 2002; Shankar et al. 2004; Marconi et al. 2004). However, the 0.16 ± 0.07

dex higher normalization of our best-fit relation for the classical bulges than the value of T02 will enhance the predicted mass and mass density of local SMBHs by $\sim 50\%$. In addition, the steeper slope of the relation for the core galaxies will raise the mass function of the most massive black holes in the universe, while the lower relation for the pseudobulges will reduce the mass function of the low mass SMBHs in the centers of disk galaxies. Such modification will also affect estimation of the fraction of obscured AGNs, which can be tested independently by the observations of cosmic hard X-ray background. We will elaborate these implications in the subsequent papers.

The significant lower normalization and shallower slope of the $M_{\text{bh}}-\sigma_*$ relation for pseudobulges appears not due to the effect of selection bias. At a give velocity dispersion, the SMBHs with massive M_{bh} are easier to be discovered and measured, because they possess larger radius of influence spheres. Here we note unbiased estimate for parameters β and α requires larger unbiased sample (both in M_{bh} and σ_*), or one must determine the selection bias carefully (e.g. Lauer et al. 2007b).

Another interesting and unexpected finding is the agreement between the slope of $M_{\text{bh}}-\sigma_e$ relation and of the $M_{\text{bh}}-\sigma_c$ rela-

tion. T02 concluded that the earlier found discrepancy arises mostly from the different definitions of stellar velocity dispersion, but this difference in our sample is insignificant (cf. Figure 1). Our estimate of σ_c is much shallower than the previous results of FM00 and FF05. This “converged” slope will be important, and in some senses, convenient for the theoretical models and numerical simulations that try to reproduce the relation.

In stead of the assumed universal $M_{\text{bh}}-\sigma_*$ relation, the real correlation is composed of three sub-samples of SMBHs: hosted by the pseudobulges, by the normal elliptical galaxies (or classical bulges) and by the “core” elliptical galaxies. They have different slope and normalization, but similar intrinsic dispersion. The tight correlation between M_{bh} and σ_* demonstrate that the bulge formation and SMBHs fueling are closely connected, despite the type of bulges. The strong feedback due to major (“wet”) mergers is the favored mechanism responsible for the formation of the correlation for the early type galaxies and classical bulges, while the slight steeper correlation for the core galaxies is build by the dry mergers of their early type progenitors. If the SMBHs in pseudobulges grow in the same period of their host bulge formation, their tight correlation may be the result of the secular evolution. But the young stellar population of the pseudobulges and the low activity of their central AGNs indicate the formation of these SMBHs may be earlier than their host bulges. The similar slope of the relations for classical bulges and pseudobulges indicates they may experience the similar AGN feedback processes (e.g. Silk & Rees 1998; King 2003), but the SMBHs growth in pseudobulges is relatively slower than that in the classical bulges. We suggest it is due to the lower efficiency of AGN fueling by secular evolution. In conclusion, the SMBHs formation and evolution scenario in the pseudobulges deserve further exploration, especially for the early stage of disk galaxy formation.

ACKNOWLEDGMENTS

I wish to thank Rashid Sunyaev for stimulating this work. I am especially grateful to John Kormendy for helping to identify the bulge type of some galaxies. Extensive use was made of the HyperLeda database available at <http://leda.univ-lyon1.fr/>, and the NASA/IPAC Extragalactic Database, which is operated by the Jet Propulsion Laboratory, California Institute of Technology, under contract with NASA.

REFERENCES

- Akritas M. G., Bershadsky M. A., 1996, *ApJ*, 470, 706
Aller M. C., Richstone D. O., 2007, *ApJ*, 665, 120
Atkinson J. W. et al., 2005, *MNRAS*, 359, 504
Baggett W. E., Baggett S. M., Anderson K. S. J., 1998, *AJ*, 116, 1626
Balcells M., Graham A. W., Peletier R. F., 2007, *ApJ*, 665, 1084
Barth A. J., Sarzi M., Rix H.-W., Ho L. C., Filippenko A. V., Sargent W. L. W., 2001, *ApJ*, 555, 685
Barth A. J., Ho L. C., Sargent W. L. W., 2002, *AJ*, 124, 2607
Barth A. J., Greene J. E., Ho L. C., 2005, *ApJ*, 619, L151
Batcheldor D. et al., 2005, *ApJS*, 160, 76
Bedregal A. G., Aragón-Salamanca A., Merrifield M. R., 2006, *MNRAS*, 373, 1125
Bender R. et al., 2005, *ApJ*, 631, 280
Bentz M. C. et al., 2006, *ApJ*, 651, 775
Bertola F., Cinzano P., Corsini E. M., Rix H.-W., Zeilinger W. W., 1995, *ApJ*, 448, L13
Bian W., Gu Q., 2007, *ApJ*, 657, 159
Binney J., 1978, *MNRAS*, 183, 501
Binney J., 2005, *MNRAS*, 363, 937
Bower G. A. et al., 2001, *ApJ*, 550, 75
Bridges T. et al., 2006, *MNRAS*, 373, 157
Capetti A., Balmaverde B., 2007, *A&A*, 469, 75
Capetti A., Marconi A., Macchetto D., Axon D., 2005, *A&A*, 431, 465
Cappellari M., Verolme E. K., van der Marel R. P., Verdoes Kleijn G. A., Illingworth G. D., Franx M., Carollo C. M., de Zeeuw P. T., 2002, *ApJ*, 578, 787
Cappellari M. et al., 2006, *MNRAS*, 366, 1126
Cappellari M. et al., 2007a, *MNRAS*, 379, 418
Cappellari M. et al., 2007b, *astro-ph/0709.2861*
Cid Fernandes R., Gu Q., Melnick J., Terlevich E., Terlevich R., Kunth D., Rodrigues Lacerda R., Joguet B., 2004, *MNRAS*, 355, 273
Coccato L., Sarzi M., Pizzella A., Corsini E. M., Dalla Bontà E., Bertola F., 2006, *MNRAS*, 366, 1050
Copin Y., Cretton N., Emsellem E., 2004, *A&A*, 415, 889
Courteau S., McDonald M., Widrow L. M., 2007, in M. Bureau, A. Athanassoula, B. Barbuy, eds., *Proceedings of IAU Symposium No. 245 (astro-ph/0709.3682)*
Cretton N., van den Bosch F., 1999, *ApJ*, 514, 704
Curran S. J., Johansson L. E. B., Rydbeck G., Booth R. S., 1998, *A&A*, 338, 863
Dalle Ore C., Faber S. M., Gonzalez J. J., Stoughton R., Burstein D., 1991, *ApJ*, 366, 38
Davies R. I. et al., 2006, *ApJ*, 646, 754
De Francesco G., Capetti A., Marconi A., 2006, *A&A*, 460, 439
De Francesco G., Capetti A., Marconi A., 2008, *A&A*, in press (*astro-ph/0801.0064*)
Denney K. D. et al. 2006, *ApJ*, 653, 152
Devereux N., Ford H., Tsvetanov Z., Jacoby G., 2003, *ApJ*, 125, 1226
de Zeeuw P. T. et al., 2002, *MNRAS*, 329, 513
Dong X. Y., De Robertis M. M., 2006, *AJ*, 131, 1236
Drory N., Fisher D. B., 2007, *ApJ*, 664, 640
Emsellem E., Dejonghe H., Bacon R., 1999, *MNRAS*, 303, 495
Erwin P., 2007, in M. Bureau, A. Athanassoula, B. Barbuy, eds., *Proceedings IAU Symposium No. 245 (astro-ph/0709.3793)*
Erwin P., Beltrán J. C. V., Graham A. W., Beckman J. E., 2003, *ApJ*, 597, 929
Erwin P., Graham A., Caon N., 2002, preprint (*astro-ph/0212335*)
Faber S., Wegner G., Burstein D., Davies R., Dressler A., Lynden-Bell D., Terlevich R., 1989, *ApJS*, 69, 763
Fabian A., Iwasawa K., 1999, *MNRAS*, 303, L34
Fathi K., Peletier R. F., 2003, *A&A*, 407, 61
Ferrarese L., Ford H. C., 1999, *ApJ*, 515, 583
Ferrarese L., Ford H. C., 2005, *Space Sci. Rev.*, 116, 523 (FF05)
Ferrarese L., Merritt D., 2000, *ApJ*, 539, L9 (FM00)
Ferrarese L., Ford H. C., Jaffe W., 1996, *ApJ*, 470, 444
Ferrarese L., Mould J. R., Stetson P. B., Tonry J. L., Blakeslee J. P., Ajhar E. A., 2007, *ApJ*, 654, 186
Ferrarese L. et al., 2006, *ApJS*, 164, 334
Fisher D. B., 2006, in J.-P. Beaulieu, K. J. Meech eds., *Proceedings of Frank N. Bash Symposium 2005: New Horizons in Astronomy*, (San Francisco: ASP), 237
Gadotti D. A., 2007, *MNRAS*, in press (*astro-ph/0708.3870*)
Gebhardt K. et al., 2000a, *ApJ*, 539, L13

- Gebhardt K. et al., 2000b, *AJ*, 119, 1157
- Gebhardt K. et al., 2003, *ApJ*, 583, 92
- Gebhardt K. et al., 2007, *ApJ* submitted (astro-ph/0709.0585)
- Ghez A. M. et al., 2005, *ApJ*, 620, 744
- Graham A. W., 2002, *ApJ*, 568, L13
- Graham A. W., Driver S. P., 2007, *ApJ*, 655, 77
- Graham A. W., Erwin P., Caon N., Trujillo I., 2001, *ApJ*, 563, L11
- Greene J. E., Ho L. C., 2006, *ApJ*, 641, L21
- Greenhill L. J., Gwinn C. R., 1997, *Ap&SS*, 248, 261
- Greenhill L. J., Moran J. M., Herrnstein J. R., 1997, *ApJ*, 481, L23
- Greenhill L. J. et al., 2003, *ApJ*, 590, 162
- Häring N., Rix H., 2004, *ApJ*, 604, L89
- Häring-Neumayer N., Cappellari M., Rix H.-W., Hartung M., Prieto M. A., Meisenheimer K., Lenzen R., 2006, *ApJ*, 643, 226
- Harms R. J. et al., 1994, *ApJ*, 435, L35
- Herrnstein J. R. et al., 1999, *Nature*, 400, 539
- Hicks E. K. S., Malkan M. A., 2008, *ApJS*, 174, 31
- Houghton R. C. W., Magorrian J., Sarzi M., Thatte N., Davies R. L., Krajnović D., 2006, *MNRAS*, 367, 2
- Hughes M. A. et al., 2005, *AJ*, 130, 73
- Ishihara Y., Nakai N., Iyomoto N., Makishima K., Diamond P., Hall P., 2001, *PASJ*, 53, 215
- Jørgensen I., Franx M., Kjaergaard P., 1995, *MNRAS*, 276, 1341
- Karachentsev I. D. et al., 2007, *AJ*, 133, 504
- Kauffmann G. et al., 2003, *MNRAS*, 346, 1055
- King A., 2003, *ApJ*, 596, L27
- Knapen J. H., Mazzuca L. M., Böker T., Shlosman I., Colina L., Combes F., Axon D. J., 2006, *A&A*, 448, 489
- Kobulnicky H. A., Gebhardt K., 2000, *AJ*, 119, 1608
- Kondratko P. T., Greenhill L. J., Moran J. M., 2005, *ApJ*, 618, 618
- Kormendy J., 1999, in D. Merritt, J. A. Sellwood, M. Valluri eds., *Galaxy Dynamics: A Rutgers Symposium*, (San Francisco: ASP), 124
- Kormendy J., Bender R., 1999, *ApJ*, 522, 772
- Kormendy J., Fisher D. B., 2005, *Rev. Mex. AA*, 23, 101
- Kormendy J., Gebhardt K., 2001, in H. Martel J. C. Wheeler eds., *The 20th Texas Symposium on Relativistic Astrophysics*, AIP, 363,
- Kormendy J., Kennicutt Jr., R. C., 2004, *ARA&A*, 42, 603
- Kormendy J., Richstone D., 1995, *ARA&A*, 33, 581
- Kormendy J., Cornell M. E., Block D. L., Knapen J. H., Allard E. L., 2006, *ApJ*, 642, 765
- Kuntschner H. et al., 2006, *MNRAS*, 369, 497
- Lauer T. R. et al., 1995, *AJ*, 110, 2622
- Lauer T. R. et al., 2007a, *ApJ*, 662, 808
- Lauer T. R., Tremaine S., Richstone D., Faber S. M., 2007b, *ApJ*, 670, 249
- Laurikainen E., Salo H., Buta R., Vasylyev S., 2004, *MNRAS*, 355, 1251
- Laurikainen E., Salo H., Buta R., 2005, *MNRAS*, 362, 1319
- Lodato G., Bertin G., 2003, *A&A*, 398, 517
- Lütticke R., Dettmar R.-J., Pohlen M., 2000, *A&AS*, 145, 405
- Macchetto F., Marconi A., Axon D. J., Capetti A., Sparks W., Crane P., 1997, *ApJ*, 489, 579
- Magorrian J. et al., 1998, *AJ*, 115, 2285
- Marconi A., Hunt L. K., 2003, *ApJ*, 589, L21
- Marconi A., Risaliti G., Gilli R., Hunt L. K., Maiolino R., Salvati M., 2004, *MNRAS*, 351, 169
- Martini P., Regan M. W., Mulchaey J. S., Pogge R. W., 2003, *ApJS*, 146, 353
- Mei S. et al., 2007, *ApJ*, 655, 144
- Merritt D., Ferrarese L., 2001, *ApJ*, 547, 140
- McLure R. J., Dunlop J. S., 2002, *MNRAS*, 331, 795
- Muñoz Marín V. M. et al., 2007, *AJ*, 134, 648
- Neistein E., Maoz D., Rix H.-W., Tonry J. L., 1999, *AJ*, 117, 2666
- Nelson C. H., Whittle M., 1995, *ApJS*, 99, 67
- Nelson C., Green R., Bower G., Gebhardt K., Weistrop D., 2004, *ApJ*, 615, 652
- Novak G. S., Faber S. M., Dekel A., 2006, *ApJ*, 637, 96
- Nowak N., Saglia R. P., Thomas J., Bender R., Pannella M., Gebhardt K., Davies R. I., 2007, *MNRAS*, 379, 909
- Oosterloo T. A. et al., 2007, *New Astronomy Reviews*, 51, 8
- Ott M., Whiteoak J. B., Henkel C., Wielebinski R., 2001, *A&A*, 372, 463
- Pastorini G. et al., 2007, *A&A*, 469, 405
- Peletier, R. F. et al., 2007, *MNRAS*, 379, 445
- Peterson B. M. et al., 2004, *ApJ*, 613, 682
- Press W. H., Teukolsky S. A., Vetterling W. T., Flannery B. P., 1992, *Numerical Recipes* (2d ed.; Cambridge: Cambridge Univ. Press)
- Prugniel Ph., Héraudeau Ph., 1998, *A&AS*, 128, 299
- Rejkuba M., 2004, *A&A*, 413, 903
- Richstone D. et al., 2004, preprint (astro-ph/0403257)
- Rix H.-W., Carollo C. M., Freeman K., 1999, *ApJ*, 513, L25
- Saglia R. P., Kronawitter A., Gerhard O., Bender R., 2000, *AJ*, 119, 153
- Sarzi M., Rix H.-W., Shields J. C., Rudnick G., Ho L. C., McIntosh D. H., Filippenko A. V., Sargent W. L. W., 2001, *ApJ*, 550, 65
- Scarlata C. et al., 2004, *AJ*, 128, 1124
- Schinnerer, E., Eckart A., Tacconi L. J., 2000, *ApJ*, 533, 826
- Shankar F., Salucci P., Granato G. L., De Zotti G., Danese L., 2004, *MNRAS*, 354, 1020
- Shapiro K. L., Cappellari M., de Zeeuw T., McDermid R. M., Gebhardt K., van den Bosch R. C. E., Statler T. S., 2006, *MNRAS*, 370, 559
- Shapiro K. L., Gerssen J., van der Marel R. P., 2003, *AJ*, 126, 2707
- Shaw M., Wilkinson A., Carter D., 1993, *A&A*, 268, 511
- Silge J. D., Gebhardt K., Bergmann M., Richstone D., 2005, *AJ*, 130, 406
- Silk J., Rees M. J., 1998, *A&A*, 331, L1
- Simien F., Prugniel P., 1998, *A&AS*, 131, 28
- Soltan A., 1982, *MNRAS*, 200, 115
- Tadhunter C., Marconi A., Axon D., Wills K., Robinson T. G., Jackson N., 2003, *MNRAS*, 342, 861
- Thornton R. J., Stockton A., Ridgway S. E., 1999, *ApJ*, 118, 1461
- Tonry J. L., Dressler A., Blakeslee J. P., Ajhar E. A., Fletcher A. B., Luppino G. A., Metzger M. R., Moore C. B., 2001, *ApJ*, 546, 681
- Tremaine S. et al., 2002, *ApJ*, 574, 740 (T02)
- Treu T., Malkan M. A., Blandford R. D., 2004, *ApJ*, 615, L97
- Treu T., Woo J.-H., Malkan M. A., Blandford R. D., 2007, *ApJ*, 667, 117
- Valluri M., Merritt D., Emsellem E., 2004, *ApJ*, 602, 66
- van den Bosch F. C., van der Marel R. P., 1995, *MNRAS*, 274, 884
- Verolme E. K. et al., 2002, *MNRAS*, 335, 517
- Wegner, G. et al., 2003, *AJ*, 126, 2268
- Wilson A. S., Shopbell P. L., Simpson C., Storchi-Bergmann T., Barbosa F. K. B., Ward M. J., 2000, *AJ*, 120, 1325
- Wold M., Lacy M., Käuff H. U., Siebenmorgen R., 2006, *A&A*, 460, 449

- Woo, J.-H., Treu T., Malkan M. A., Blandford R. D., 2006, ApJ, 645, 900
Wyithe J. S. B., 2006, MNRAS, 365, 1082
Wyithe J. S. B., Loeb A., 2003, ApJ, 595, 614
Yamauchi A., Nakai N., Sato N., Diamond P., 2004, PASJ, 56, 605
Yu Q., Tremaine S., 2002, MNRAS, 335, 965

This paper has been typeset from a $\text{T}_{\text{E}}\text{X}/\text{L}^{\text{A}}\text{T}_{\text{E}}\text{X}$ file prepared by the author.